Supporting Information

Multichannel Linear and Nonlinear Information Encryptions with Malus Metasurfaces

Yuexin Sun, Guangzhou Geng, Yanchun Wang, Yuebian Zhang*, Zhancheng Li, Wenwei Liu, Hua Cheng*, Shuqi Chen*

S1. Linear and nonlinear optical properties of the polarization decoupling metasurface

The simulated reflection spectra of the polarization decoupling metasurface consisting of uniformly distributed structures under the illumination of left-handed circularly polarized (LCP) fundamental wave are shown in Figure S1a. The circular polarization can be decomposed into a pair of orthogonal linear polarizations parallel and perpendicular to the base of split-ring resonators (SRRs), and only the one parallel to the base can couple with structures and induce circulating currents that lead to magnetic resonance. The magnetic dipole mode is located at the wavelength of 1400 nm, consistent with the result of the linearly polarized light shown in Figure 2a. Figure S1b shows the corresponding second harmonic (SH) intensity as a function of the fundamental wavelength, with the strongest SH intensity at the wavelength of approximately 1400 nm. The hydrodynamic model was utilized during the simulation to study the SH process.[1-3]
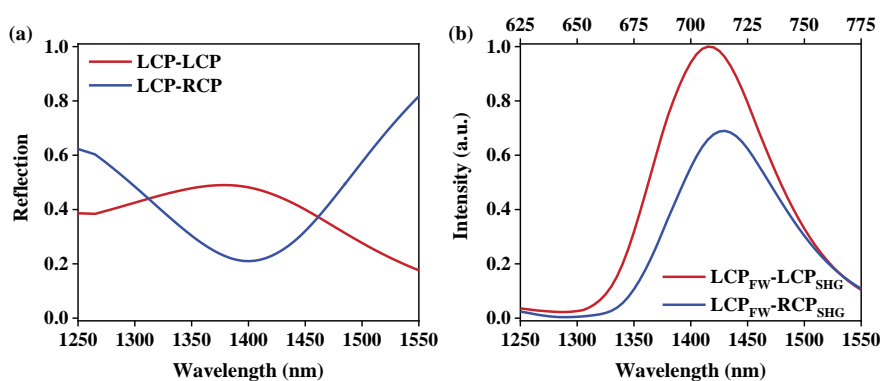

Figure S1. (a) Simulated linear reflection spectra and (b) SH intensity of the polarization decoupling metasurface.

S2. Polarization ellipses of SRRs with different wavelengths and orientation angles

Polarizations of the fundamental and SH wave channels can be decoupled using the metasurface

composed of SRRs. As shown in Figure 2c, the polarization ellipses of the structure at the wavelength of 1550 nm have different main axis directions and ellipticities in different frequency channels, which provides a means for multichannel polarization encryption. Based on the electric field simulated by COMSOL multiphysics, the calculated polarization ellipses of the two frequency channels with different wavelengths are presented in Figure S2a. It can be seen that the major axis direction of the polarization state of the fundamental channel varies with the wavelength, while that of the SH wave channel is almost constant. The angle between the major axes of the fundamental and SH wave channels varies with the wavelength, which indicates the potential of the metasurface for polarization decoupling of different channels. It can be seen that the intersection angles between the major axes of the fundamental and SH wave channels increase when the wavelength is far away from the resonant wavelength (1400 nm). Furthermore, the polarization ellipses of structures with different orientation angles are calculated when the incident wavelength is 1550 nm, as structures with different orientation angles are utilized to achieve distinct intensity distributions in two channels. As shown in Figure S2b, the ellipticity of the polarization ellipse remains nearly unchanged for both frequency channels as the rotation angle varies, while the direction of the major axis rotates with the rotation of structures. Moreover, the major axis of the polarization state of the SH wave channel is almost oriented along the short arm of the SRR, resulting in the minimum intensity located at approximately 90º, as shown in Figures 2d and 2e.
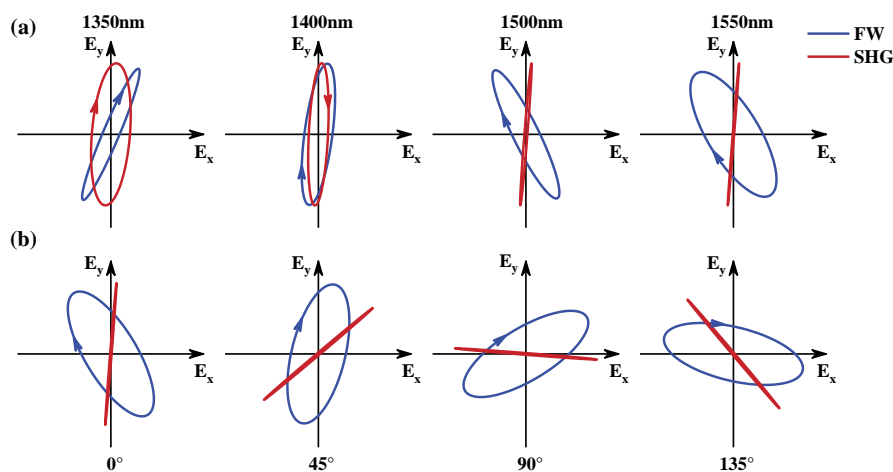
Figure S2. Calculated polarization ellipses for different channels. (a) The polarization ellipses of the structures with different wavelengths. (b) The polarization ellipses of the structures with different orientation angles for the fundamental wave (blue lines) and SH wave (red lines) channels.

S3. Robustness of the polarization state of the fundamental wave channel to the structure size

The relative position between the working wavelength and the resonant wavelength depends on the selection of structural parameters, which will inevitably be affected by fabrication errors. To evaluate the impact of fabrication errors on the polarization state of the fundamental wave channel, we calculated the variation of the polarization state with two main parameters w and L_y, as shown in Figure S3. The deviations of these two parameters from their optimal values are represented by δw and δL_y. The polarization state is characterized by the direction of the major axis ψ and the ellipticity χ of the polarization ellipse. It can be seen that the direction of the major axis ψ changes slightly with the variation of the parameters, while the variation of the ellipticity χ of the polarization ellipse is more obvious. Thus, within the fabrication error range of ±10 nm, grayscale images in different frequency channels can still be distinguished for the inconspicuous change of the major axis ψ, but the image contrast will be lower due to the evident changes in the ellipticity χ.
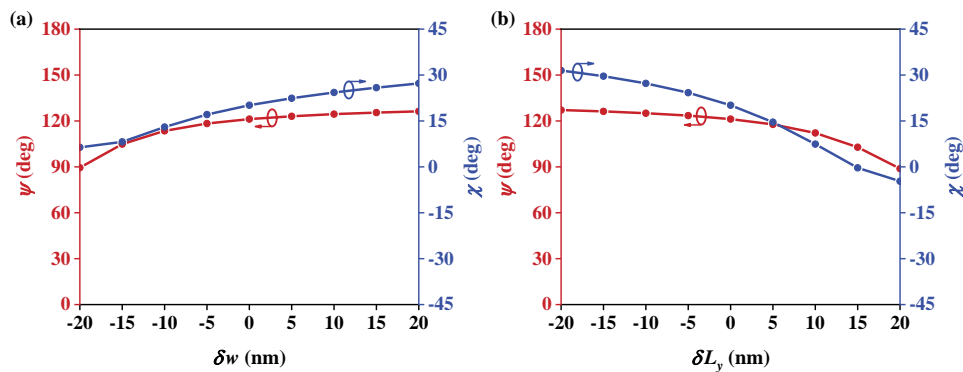

Figure S3. Calculated polarization states of the fundamental wave channel as functions of

structure parameter variations. (a) The variation of the polarization ellipse with the width difference δw. (b) The variation of the polarization ellipse with the short arm length difference δL_y, while keeping the w unchanged.

S4. Linear and nonlinear optical properties of the tri-channel nonlinear metasurface

The simulated linear reflection spectra and the generating nonlinear intensity as functions of the incident fundamental wavelength of the tri-channel nonlinear metasurface, which is used to implement a grayscale image in the near field and two holograms in the far field, are shown in Figure S4. This metasurface was optimized to resonate at the laser operating wavelength (1550 nm) to improve the nonlinear conversion efficiency. The long arm length L_x is 220 nm, the short arm length L_y is 118 nm, the arm width w is 55 nm, and other parameters are the same as those proposed previously.
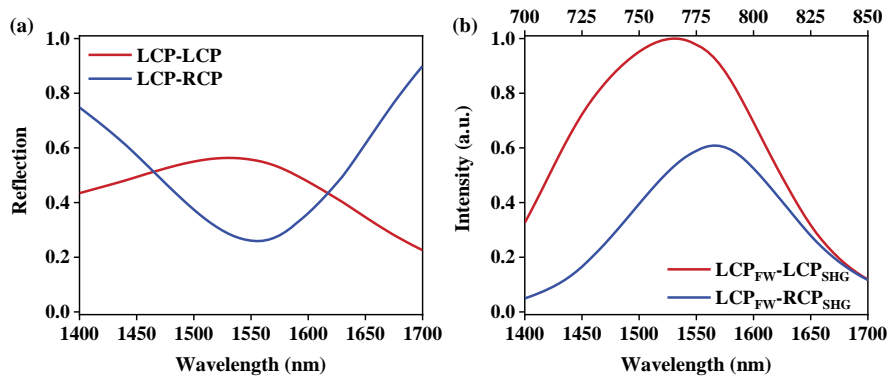

Figure S4. (a) Simulated linear reflection spectra and (b) SH intensity of the tri-channel nonlinear metasurface.

S5. Flow chart of the modified Gerchberg–Saxton (GS) algorithm

The GS algorithm has been widely used in metasurfaces to reconstruct holograms in real space and k-space. Firstly, the distribution of orientation angles can be calculated based on the GS algorithm. Then, holographic images can be constructed in the far field by the Fourier transform (FT).

We employ the modified GS algorithm to simultaneously construct two holographic images with different polarizations in the far field and encrypt a grayscale image in the near field. The

modified part is the mean square error (*MSE*) added during the iteration as the acceptance criterion, through which the crosstalk between the $\exp(i\theta)$ and $\exp(i3\theta)$ can be released, and the quality of the constructed images can be remarkably improved. First, random phase distributions $\exp(i\varphi_a)$ and $\exp(i\varphi_b)$ are multiplied with the target amplitude distributions as initial envelopes for two channels to transform. After an inverse Fourier transform (IFT), the complex amplitude distributions $A_0{}'\exp(i\varphi_1)$ and $B_0{}'\exp(i\varphi_2)$ at the metasurface plane are obtained. Subsequently, the phase of different channels can be derived, which can be used to optimize the phase distribution θ_n of the metasurface. Choosing φ_1 as the initial phase distribution to start the iteration, the amplitude constraint is applied to attach the amplitude of the grayscale image. Then, the complex amplitude distributions of two channels are transformed into the hologram plane, and the acceptance criterion c_0 is calculated as the initial value. In the next step, changing one element in the phase matrix (θ_n), the phase distribution is changed if the criterion is satisfied, else the phase distribution is the same as the last loop. Repeat the loop until all elements in the phase matrix are assessed. Finally, different holographic images can be reconstructed at different polarization channels.
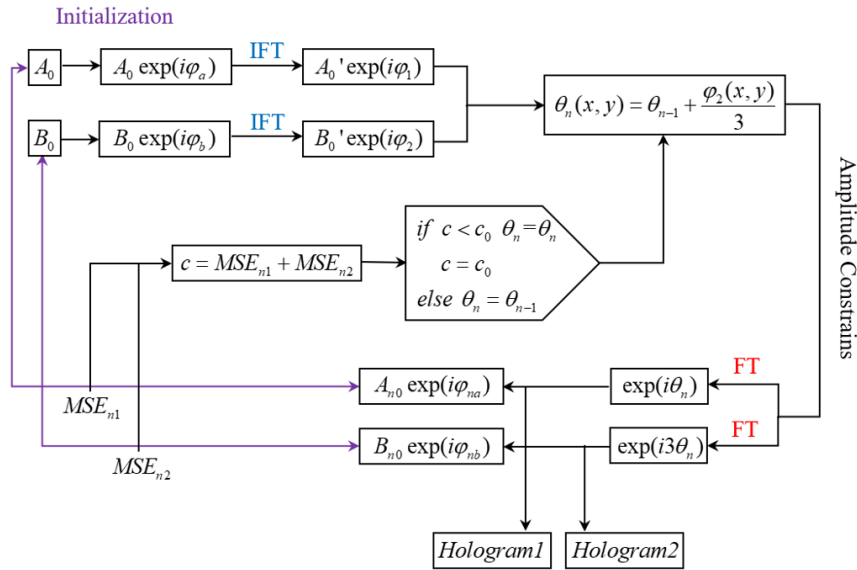

Figure S5. Flow chart of the modified GS algorithm for encoding two holograms with different polarizations. A_0 and B_0 represent the target amplitude distributions of holograms for two

channels with different polarizations. The phase distribution of metasurface θ_n is related to the rotation angle of unit cells, whose initial value θ_0 is φ_1. MSE_{n1} and MSE_{n2} are introduced to describe the difference between the amplitude distributions after each iteration and the target amplitude distributions.

S6. Variations of the amplitude and phase shift of the SH signal with the rotation angle

Figure S6a proves that the amplitude of the generated SH signals is little affected by the rotation angle. Besides, based on the nonlinear selection rule, for SRRs with C_1 rotation symmetry, the SH signal with the polarization of LCP has a phase shift of 3θ, while the phase shift of the right-handed circularly polarized (RCP) SH signal is θ, as shown in Figure S6b.
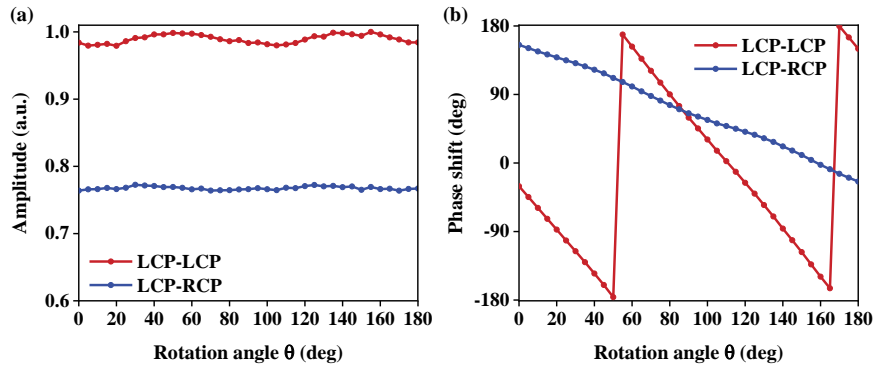
Figure S6. (a) The amplitude variation and (b) The phase shift of the generated SH signal with the rotation angle.

S7. Extended strategy of simultaneously encoding continuous and binary grayscale images

Encoding the continuous and binary grayscale images on two frequency channels can be simultaneously achieved by a single metasurface with dissimilar types of structures. The fundamental polarization state of the SRR is elliptical with its major axis along the vertical direction under LCP incidence at the resonant wavelength, which maintains the characteristic of continuous intensity change. The polarization state of the nanorod is almost linear and along the long axis under the electric dipole resonance condition. Consequently, the intensities of the fundamental wave of both structures can be approximately equal by optimizing the structural parameters, as shown in Table S1. The nanorod with two-fold rotational symmetry does not

allow the SH process based on the selection rules for harmonic generation of circular polarized fundamental waves,[4] so it behaves as "0" in the SH wave channel. The SH signals can be generated by SRRs and decomposed into a pair of orthogonal circular polarization states. Therefore, we can encode a continuous grayscale pattern with either SRRs or nanorods. The structure selection depends on the binary pattern of the SH wave channel. Specifically, when "0" is needed for the SH wave channel, the nanorod is selected, while the SRR can be used to achieve "1". In this method, a circular polarizer is critical in decoding the binary pattern on the SH wave channel. When the output light is filtered by a circular polarizer, a binary intensity distribution can be achieved.

Table S1. Intensity distribution of different structures in different frequency channels

Type of structure	Intensity of the fundamental wave channel	Intensity of the SH wave channel
(nanorod)	(sinusoidal wave)	0
(split-ring resonator)	(sinusoidal wave)	1

References:

[1] C. Ciracì, E. Poutrina, M. Scalora, D. R. Smith, *Phys. Rev. B* **2012**, *86*, 115451.

[2] Z. Hao, W. Liu, Z. Li, Z. Li, G. Geng, Y. Wang, H. Cheng, H. Ahmed, X. Chen, J. Li, J. Tian, S. Chen, *Laser Photonics Rev.* **2021**, *15*, 2100207.

[3] X. Zhang, J. Deng, M. Jin, Y. Li, N. Mao, Y. Tang, X. Liu, W. Cai, Y. Wang, K. Li, Y. Liu, G. Li, *Sci. China Phys. Mech.* **2021**, *64*, 294215.

[4] G. Li, S. Chen, N. Pholchai, B. Reineke, P. W. Wong, E. Y. Pun, K. W. Cheah, T. Zentgraf, S. Zhang, *Nat. Mater*. **2015**, *14*, 607.